Separation Science and Technology
Publication details, including instructions for authors and subscription information:
http://www.informaworld.com/smpp/title~content=t713708471

PURE GAS PERMEABILITIES OF A SERIES OF SUBSTITUTED BISPHENOXY PHOSPHAZENE POLYMERS

Mark L. Stone[a]; Fred J. White[a]; Frederick F. Stewart[a]; Marilyn N. Tsang[a]; Christopher J. Orme[a]; Eric S. Peterson[a]
[a] Idaho National Engineering and Environmental Laboratory, Idaho Falls, Idaho, U.S.A.

Online publication date: 30 June 2001

To cite this Article Stone, Mark L. , White, Fred J. , Stewart, Frederick F. , Tsang, Marilyn N. , Orme, Christopher J. and Peterson, Eric S.(2001) 'PURE GAS PERMEABILITIES OF A SERIES OF SUBSTITUTED BISPHENOXY PHOSPHAZENE POLYMERS', Separation Science and Technology, 36: 5, 1067 — 1084
To link to this Article: DOI: 10.1081/SS-100103637
URL: http://dx.doi.org/10.1081/SS-100103637

SEPARATION SCIENCE AND TECHNOLOGY, 36(5&6), 1067–1084 (2001)

PURE GAS PERMEABILITIES OF A SERIES OF SUBSTITUTED BISPHENOXY PHOSPHAZENE POLYMERS

Mark L. Stone, Fred J. White, Frederick F. Stewart, Marilyn N. Tsang, Christopher J. Orme, and Eric S. Peterson

Idaho National Engineering and Environmental Laboratory, P.O. Box 1625, Idaho Falls, Idaho 83415-2208

ABSTRACT

Polyphosphazenes are a class of inorganic polymers characterized by the phosphorus nitrogen repeating unit that forms the backbone. The phosphorus is pentavalent and the backbone has alternating single and double bonds. This leaves two coordination sites on the phosphorus free for substituted with a variety of nucleophilic groups. Several hundred polyphosphazene formulations have been reported in the literature. The ease of controlling the type and number of substituents provides a unique opportunity to develop special series of polymers to investigate structure property relationships. In this paper the pure gas permeabilities of a series of substituted bisphenoxyphosphazene polymers is reported. The polymers were exposed to ten different gases and the resulting permeabilities were analyzed using the time lag method. The time lag method enables the permeability to be broken down into its solubility and diffusivity components. Careful examination of the results makes it possible to determine what types of substituent-gas interactions are responsible for the overall permeabilities in the polymers. Some of

the polymers showed low permeabilities for all of the test gases, while others showed very large differences among the different gases tested. Especially interesting differences were observed for the series of alkanes tested. The results permit the prediction of what types of mixed gas separations might be worth pursuing.

INTRODUCTION

Energy efficient separations are an ever increasing need in the world today. This need has prompted a large increase in the efforts to develop polymeric membranes (1). The clear needs are for materials that can withstand the harsh environments of the separation process while at the same time perform the desired separations with higher efficiencies. Efforts are underway to elucidate the mechanisms of transport in various materials. A precise understanding of the intermolecular interactions occurring during the transport of a permeating molecule (gas or liquid), through a polymer will hopefully lead to the ability to not only predict the performance of a material, but actually make it possible to design a polymer that will have the desired characteristics.

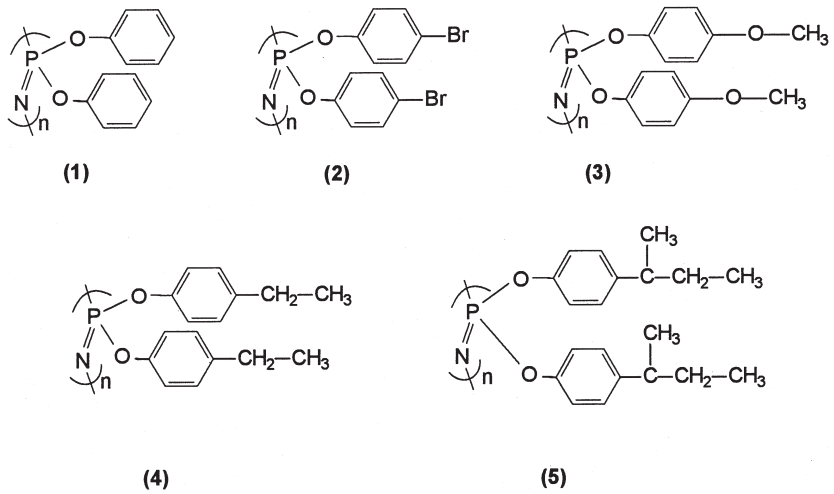

(1) Poly(bisphenoxy) phosphazene
(2) Poly(bis-*p*-bromophenoxy) phosphazene
(3) Poly(bis-*p*-methoxyphenoxy) phosphazene
(4) Poly(bis-*p*-ethylphenoxy) phosphazene
(5) Poly(bis-*p*-*sec*-butylphenoxy) phosphazene

Figure 1. Structures and names of the polymers.

MARCEL DEKKER, INC.
270 Madison Avenue, New York, New York 10016

To study the structure-separation correlation in polymeric membranes a series of polyphosphazene membranes have been synthesized. Polyphosphazenes are uniquely suited for this type of study because of their easily altered chemical structures (2). A phosphazene unit is a doubly bonded phosphorus-nitrogen monomer. Each monomer is singly bonded to both neighbors. Additionally, the pentavalent phosphorus atoms have two coordination sites at which a wide variety of substituents can be attached (3,4). Thus it is possible to synthesize closely related series of polymers such that performance and property changes are directly correlated to the pendant groups. This arrangement permits the systematic study of the correlation between the structures and transport properties of the polymers.

In this paper, a systematic series of substituted bisphenoxy phosphazene materials were synthesized, characterized, and their permeation properties measured. The structures of the materials studied are shown in Fig. 1.

EXPERIMENTAL

Polymer Synthesis

The general procedure for preparing the polymers consisted of a ring opening polymerization to form the backbone, followed by ligand substitution (Fig. 2). The linear polymers used in this study were produced using the following procedure (5).

1. Hexachlorocyclotriphosphazene was polymerized under vacuum at 250°C for 24 to 48 h.
2. The polymerized material was dissolved in toluene and purified by precipitation into hexane.
3. The pure poly(dichlorophosphazene) was dissolved in dry toluene and added to tetrahydrofuran (THF) + diglyme solution containing 20 mole percent excess sodium aryloxide. (Mole percentages are based on the number of moles of chlorine in poly(dichlorophosphazene.) Aryloxides of varying phenols were synthesized by application of sodium metal or sodium hydride in THF.
4. This solution was refluxed at approximately 115°C for 42 h. THF was removed using a Dean-Stark trap until a constant reflux temperature of 115°C was achieved.

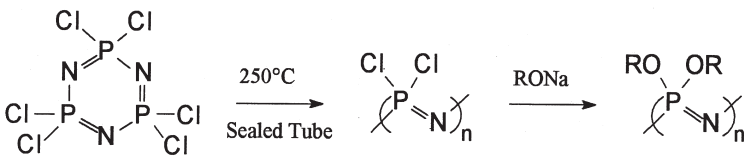

Figure 2. Reaction pathway to polyphosphazene materials.

5. After cooling, the reaction mixture was precipitated into a large excess of methanol.
6. The solids were separated by filtration and were washed with water and methanol to remove occluded sodium chloride and excess phenols.
7. The polymer was purified by dissolving it in tetrahydrofuran followed by precipitation into a large excess of water.
8. Air-drying was done for 12 h, followed by vacuum drying for 2 days.

Time-Lag Method

The permeation results were obtained using the time-lag method (6,7,8) in which each material was exposed to eleven different gases. The observed behavior of the transport of the gases through the membranes was interpreted using the solution-diffusion approach. This process consists of three steps, 1) the gas or vapor dissolves at one surface, 2) diffuses through the film due to the concentration gradient, and 3) desorbs out of the membrane on the low pressure side. In a typical experiment, both sides of the membrane are evacuated to an equal vacuum. The cell is then isolated and the zero time pressure is noted. Next, the feed side is exposed to the test or challenge gas. Finally the pressure build up on the permeate side is recorded as a function of time. The following derivation follows closely that given by Rogers (6). Initially there is a nonlinear pressure increase, but at a later time a steady state will be reached and the gas will diffuse through the film at a constant rate. Fick's first law describes what happens during this steady state (q or the flux is constant; the straight line portion of the curve—see Fig. 3.) It is then possible to relate the slope of the straight line portion of the experimental curve to the permeability of the membrane.

$$q = -D\frac{dc}{dx} \tag{1}$$

q is the amount of gas diffusing through a unit area per unit of time or the FLUX, D is the diffusion constant, and dc/dx is the change in concentration of the solute within the film or the concentration gradient across thickness dx.
Rewriting, integrating with D independent of c, and rearranging gives

$$qdx = -Ddc \rightarrow q\int_0^l dx = -D\int_{c1}^{c2} dc \rightarrow q = \frac{D(c_1 - c_2)}{l} \tag{2}$$

Gas concentrations are normally measured in terms of pressure, p, of the gas at equilibrium with the film. According to Henry's law we have

$$c = Sp \tag{3}$$

where S is the Henry's law solubility constant, c is the concentration of the dissolved gas in the film, and p is the pressure of the gas applied to the membrane

MARCEL DEKKER, INC.
270 Madison Avenue, New York, New York 10016

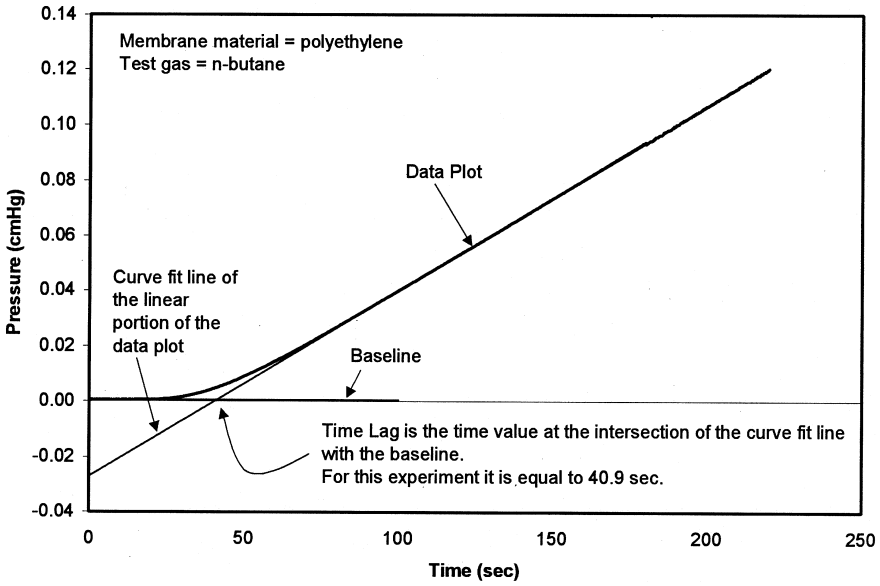

Figure 3. An illustration of how the time lag data is displayed and the parameters evaluated.

surface. So,

$$q = \frac{D(Sp_1 - Sp_2)}{l} = \frac{DS(p_1 - p_2)}{l} \tag{4}$$

The permeability is defined as

$$P \equiv DS = \frac{ql}{(p_1 - p_2)} = (\text{flux} \times \text{thickness})/(\text{permeant pressure difference}) \tag{5}$$

where the permeant pressure difference is the concentration (pressure) of the permeant in the feed (p_1) minus the concentration of the permeant in the permeate (p_2). In the above equation q is the amount of gas transmitted at the steady state in unit time through unit area of film. From a plot of the increase in pressure at the low-pressure (permeate) side versus time after the steady state has been established $\Delta p/\Delta t$ (the slope) can be obtained. The Δp (in cm Hg) has to be converted to a volume of the permeate gas at STP. During the experiment the pressure is measured, the experimental volume is measured, and the experimental temperature is recorded.

So the volume of permeate gas (converted to STP conditions; pressure in cm Hg) per unit of time that goes through the membrane is given by (rearranging

terms and dividing both sides by Δt)

$$\frac{V_{STP}}{\Delta t} = \frac{\Delta p}{\Delta t} * \frac{V_{system}}{76} * \frac{273}{(273 + T)} = slope * \frac{V_{system}}{76} * \frac{273}{(273 + T)} \tag{6}$$

Since q is volume per unit time per unit of area (A in cm^3)

$$q = \frac{V_{STP}}{\Delta t} + A = slope * \frac{V_{system}}{76} * \frac{273}{(273 + T)} * \frac{1}{A} \tag{7}$$

Substituting this into the permeability equation above gives

$$P = slope * \frac{V_{system}}{76} * \frac{273}{(273 + T)} * \frac{1}{A} * \frac{l}{(p_1 - p_2)} \tag{8}$$

It is important to recognize that there are two pressure quantities involved in these calculations. The (p_1-p_2) term in the denominator is the driving force term. All of the feed side pressure is due to the permeant so the p_1 term is the measured pressure. The permeate pressure is purposely kept at a very low (usually $< 0.1\%$ of the feed pressure). Thus, this term can be ignored.

The other pressure involved is the pressure change per unit of time and is used to calculate a slope value for $\Delta p/\Delta t$. The final equation for the permeability is (V_{system} in cm^3, the slope in cmHg/sec, and $p_1$in cmHg)

$$P = slope * \frac{V_{system}}{76} * \frac{273}{(273 + T)} * \frac{1}{A} * \frac{l}{p_1} \tag{9}$$

Non-Steady State Conditions

At the very beginning of a pure gas experiment there is a period of time wherein the flux is changing with time. In order to relate the flux to the change in concentration, consider the situation illustrated in Fig. 4. Flow of solute or per-

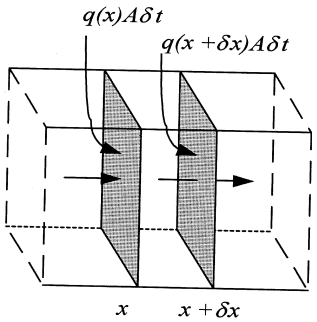

Figure 4. Conceptual flow model.

meant is occurring in the x direction in a cell of uniform cross section A. We want to calculate the change in concentration in a thin slab of thickness δx The quantity of material crossing the plane at x in time δt is $q(x)A\delta t$, whereas the quantity leaving through the plane $x + \delta x$ in the same time is $q(x + \delta x)A\delta t$, which may be written as

$$\left(q(x) + \frac{\partial q}{\partial x}\,\delta x\right) A\ \delta t \tag{10}$$

The net gain in the quantity of material between these hypothetical planes may be expressed in terms of the change of concentration in the volume $A\delta x$ or in terms of the differences between these two quantities of materials transported.

$$A\delta c\delta x = qA\delta t - \left(q + \frac{\partial q}{\partial x}\,\delta x\right) A\delta t = -\frac{\partial q}{\partial x}\,A\delta x\delta t \tag{11}$$

Which in the limit, as the distances and times are made smaller gives

$$\frac{\partial c}{\partial t} = -\frac{\partial q}{\partial x} \tag{12}$$

If q is defined by Fick's law and is substituted into the above equation

$$\frac{dc}{dt} = \frac{d}{dx}\left(D\,\frac{dc}{dx}\right) \tag{13}$$

If D is independent of concentration this becomes (Fick's second law)

$$\frac{dc}{dt} = D\,\frac{d^2c}{dx^2} \tag{14}$$

A general solution to this equation has not been found for the case where D is dependent upon concentration. However, a solution for the case of a finite solid with a concentration independent diffusion constant has been worked out (7,9). This is the case where the film is initially free from gas and one surface is then exposed to gas at a pressure p_1 giving a concentration in the surface layer of c_1 and the other surface held to zero concentration, i.e., the boundary conditions are: $c = c_1$ at $x = 0$ for all values of time t, $c = 0$ at $x = l$ for all values of time t, and $c = 0$ at $x > 0$ and $\leq l$ for $t = 0$.

The concentration in the feed side membrane surface ($x = 0$) is equal to the feed concentration c_1 for the entire experiment. The concentration at the permeate side is so small in comparison to the feed side that it is considered 0. Also the concentration of the gas within the membrane is so small compared with the feed side that it is also considered to be 0. After differentiating, letting q=l, and then integrating, the solution becomes

$$q = \frac{Dc_1}{l}\,t - \frac{c_1}{6} \tag{15}$$

This indicates that q increases in a linear fashion with the time t in the steady state portion of the curve. If one now extrapolates back to linear portion to the time axis, one obtains an intercept $t = \tau$ where $q = 0$, and then solving for D gives

$$D = \frac{l_2}{6\tau} \tag{16}$$

τ (sometimes designated as θ) is known as the time lag.
UNITS: P is usually expressed in units of cc of gas at STP passing per second under gradient of 1 cm Hg per cm thickness and per square centimeter of area [($cm^3_{gas\text{-}STP}$*cm)/(sec*cm^2*cmHg)], or as Barrers = 10^{10} x [($cm^3_{gas\text{-}STP}$*cm)/(sec*cm^2*cmHg)]. D is in centimeters squared per second (cm^2/sec). S is cm^3 gas at STP per cm^3 of polymer at 1 atm pressure [(cm^3_{gas})/($cm^3_{polymer}$*atm)], so converting to atmospheres gives

$$S = \frac{76P}{D} \tag{17}$$

Just before the introduction of the test gas, a pressure reading is taken to determine the baseline pressure reading for the experiment. A line parallel to the x-axis through the baseline pressure value is drawn. After the experimental run, a plot is made showing the data, the baseline, and a line fitted to the steady state portion of the data. The fitted line is extrapolated back so that it intercepts the baseline. The time from the start of the run to the point of intersection of the baseline with the fitted line is the time lag (τ). In one such experiment, the information is given in Fig. 3. The time lag is calculated by inserting into the equation for the fitted line, the value of the baseline, and solving for the x (time) value. Thus, P and D come from the data and S is calculated from equation 17.

The glass transition temperatures (T_g) were determined using a TA Instruments Differential Scanning Calorimeter DSC Model 2910. Milligram samples were sealed in aluminum pans and cooled to –150°C. Then they were heated at 10°C/min up to 200°C. The molecular weights were measured by using light scattering (Wyatt Technology Corp., Dawn DSP Laser Photometer) and gel permeation chromatography (Waters 2690 Separations Module, Visotek 50A Differential Visometer, and Rainin Dynamax Refractive Index Detector Model RI-1.)

RESULTS AND DISCUSSION

The T_gs and molecular weights of the polymers studied are listed in Table 1. The three unsubstituted PPOP materials all had T_gs within a couple of degrees of each other at approximately –1°C (2). The *p*-ethyl and *p-sec*-butyl PPOP polymers had even lower T_gs. The other two polymers are interesting in that the *p*-Br PPOP showed no detectable T_g (although a value of 10°C has been reported (10))

MARCEL DEKKER, INC.
270 Madison Avenue, New York, New York 10016

Table 1. Thermal Characterization Data for the Seven Phosphazene Polymers

Polymer	T_g °C	$T_{(1)}$ peaks °C	MW g/mol
JP225	-1	97; 131	7.5e5[a]
TE-1-51	-2	100; 127	NM[b]
TE-1-45	-1	129	NM
p-Br PPOP	none detected	43; 142	NM
p-methoxy PPOP	17	98; 118	2.89e6
p-ethyl PPOP	-17	72; 93	5.4e6[c]
p-sec-butyl PPOP	-11	none	6.69e6

[a] This value was measured by the supplier, Elf Atochem.
[b] Not measured.
[c] Average of two values.

and the *p*-methoxy PPOP had the highest of the group at 17°C. Since all of the permeability data reported in this paper was taken at 30°C, all of the polymers would be in their rubbery states for all of the measurements made.

A typical polyphosphazene DSC curve (12) is shown in Fig. 5. It shows the T_g and two other events at higher temperatures. Table 1 summarizes the T_g, $T_{(1)}$, and molecular weight values for all of the polymers. Five of the polymers had two thermal events, the TE-1-45 only showed one, and the *p-sec*-butyl PPOP showed no other thermal feature besides the T_g in the range of –150 to 200°C. All of the polymers are good film formers.

Permeability Measurements

Our laboratory has been studying the transport properties of polyphosphazene membranes for a number of years (13-17). These materials are very attractive for membrane applications because of their chemical variety and their ability to function in harsh environments. In addition, a number of investigators at other locations have looked at the gas separation properties of a number of formulations of polyphosphazenes and compared them to other high performance polymers (18-22). All of the permeability, solubility, and diffusivity data is given in Table 2.

Figure 6 reveals some interesting correlations between structure and performance of the polymers. The gases are arranged from smallest to largest kinetic diameters (11) in the order from left to right on the chart. The series of polymers illustrates plainly the solution diffusion mechanism at work. All of the unsubstituted bisphenoxy materials show very little permeability to any of the gases tested. However, with the exception of the bromo-PPOP that showed little

MARCEL DEKKER, INC.
270 Madison Avenue, New York, New York 10016

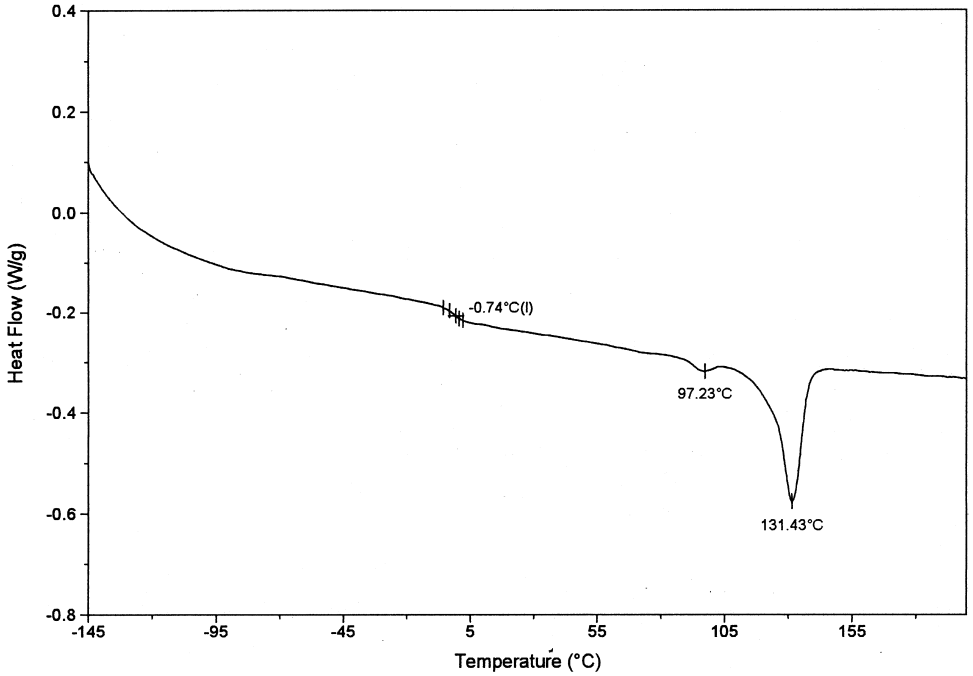

Figure 5. Typical DSC curve for a substituted phenoxyphosphazene.

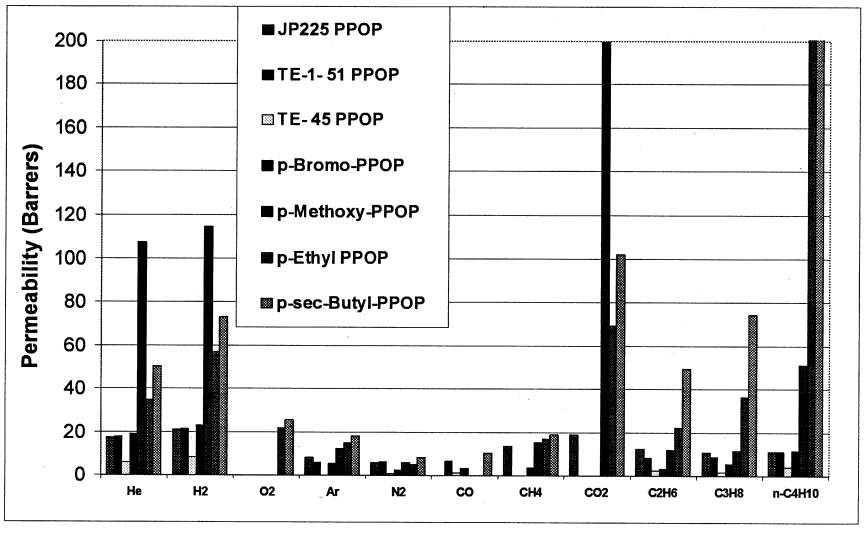

Figure 6. Permeability of seven polymers with respect to each of the test gases.

MARCEL DEKKER, INC.
270 Madison Avenue, New York, New York 10016

Table 2. Permeabilities (P), Solubilities (S), and Diffusivities (D) of the Substituted Bisphenoxy Phosphazene Membranes

		JP225 PPOP	TE-1-51 PPOP	TE-45 PPOP	p-Br PPOP	p-Methoxy PPOP	p-Ethyl PPOP	p-sec-Butyl PPOP
Helium	P	17.22		5.90	19.17	107.62	26.04	50.35
	S	0.0561		0.0230	0.2147	0.0025	0.0089	
	D	2.4E-6		2.0E-6	8.0E-7	3.9E-4	3.0E-5	
Hydrogen	P	21.21	21.55		23.20	114.36	42.38	73.34
	S	0.0362	0.5660		0.7477	0.0025	0.0150	
	D	5.9E-6	3.0E-7		2.7E-7	3.4E-4	3.0E-5	
Oxygen	P						18.02	25.52
	S						0.0602	
	D						3.63E-06	
Argon	P	8.30	5.85		5.37	12.49	12.89	18.37
	S	0.1165	0.1930		0.0346	0.0044	0.0400	0.1118
	D	5.8E-7	2.4E-7		1.2E-6	2.2E-5	3.2E-6	1.0E-6
Nitrogen	P	5.99	6.00		2.34	5.92	4.99	8.10
	S	0.0026			0.2049	0.0015	0.0198	0.0018
	D	1.7E-5			8.9E-8	2.5E-5	2.6E-6	2.9E-5
Carbon Monoxide	P				3.35			10.22
	S				0.1456			0.0137
	D				1.8E-7			6.0E-6
Methane	P	13.61			3.76	15.35	14.49	19.03
	S	0.0898			0.2255	0.0088	0.0903	0.2016
	D	1.2E-6			1.3E-7	8.7E-6	1.6E-6	4.8E-7
Carbon Dioxide	P	19.21				199.64	69.58	102.19
	S	0.2541					0.3137	
	D	5.8E-7					1.7E-6	
Ethane	P	12.38	8.40		3.11	11.87	37.10	49.64
	S	0.3133			0.4180	0.0375		0.2213
	D	3.0E-7			5.7E-8	2.4E-6		1.7E-6
Propane	P	10.71		1.80	5.30	11.71	39.91	74.38
	S	0.5255		1.0000		0.1001	2.2435	3.0904
	D	1.6E-7		1.4E-8		8.9E-7	1.5E-7	2.0E-7
Butane	P	11.04	11.25	4.30	11.46	51.13	222.07	843.14
	S	1.5718	8.2000	4.7300	5.5001	0.4514	18.7293	
	D	6.0E-8	1.2E-8	7.0E-9	1.6E-8	8.7E-7	9.0E-8	

Units: Temperature = 30°C: Feed Pressure = 30 psig
Permeability is in units of barrers = 10^{10} * ($cc_{gas\text{-}STP}$ * cm) / (sec * cm^2 * cmHg)
Solubility is = cc of gas at STP per cc of polymer at 1 atm pressure = 76 * P / D
Diffusivity = cm^2 / sec

MARCEL DEKKER, INC.
270 Madison Avenue, New York, New York 10016

difference from the parent compounds, the substitution of the phenoxy groups causes an increase in the permeation of the smallest molecules, helium and hydrogen. Gases with larger kinetic diameters, oxygen, nitrogen and carbon monoxide, are apparently too large to diffuse and too insoluble to penetrate the membrane. The last four substituted polymers show increasing solubilities for the last four gases which accounts for their higher permeabilities. The data in the figure also suggest possible membrane separations that might be considered. For example the *p*-ethyl PPOP and *p-sec*-butyl PPOP membranes might be used to separate butane from methane, butane from nitrogen, or carbon dioxide from either carbon monoxide or nitrogen.

Figure 7 displays the same data given in Fig. 6 except that the series axes are interchanged. It clearly shows that the unsubstituted materials have somewhat low permeabilities to all of the test gases. The addition of a para substituted bromo group did not have an effect on the permeations of these gases. Whereas the other substituted materials show the diffusion and solubility dependence of the various permeants. For example, consider *p*-ethyl PPOP with respect to helium and propane. The permeabilities are similar, 26 and 40, respectively. However the diffusivity of helium is approximately two orders of magnitude higher than that for propane. Likewise, the solubility of propane is roughly two orders of magnitude higher than that for helium. This is a good example of the interplay of the mechanism (either solubility or diffusivity) that are present in thin dense film membrane

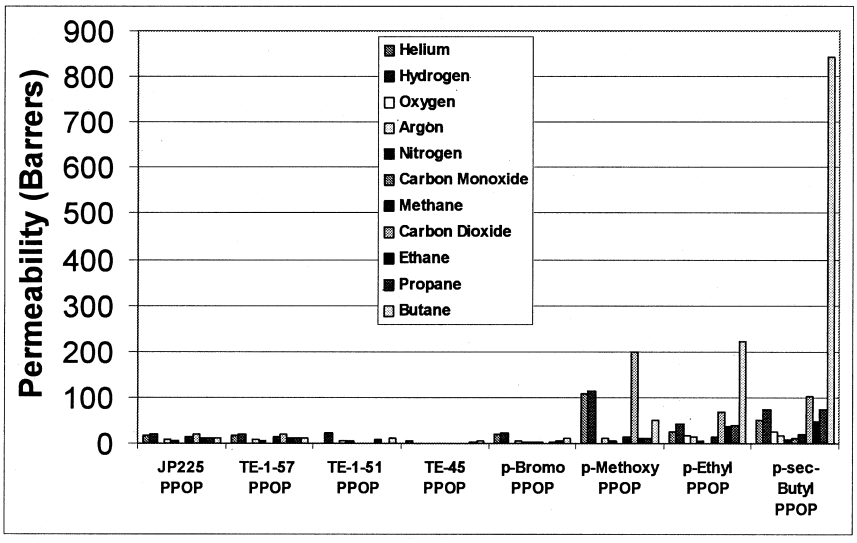

Figure 7. Permeability of the polymers with respect to the test gases.

MARCEL DEKKER, INC.
270 Madison Avenue, New York, New York 10016

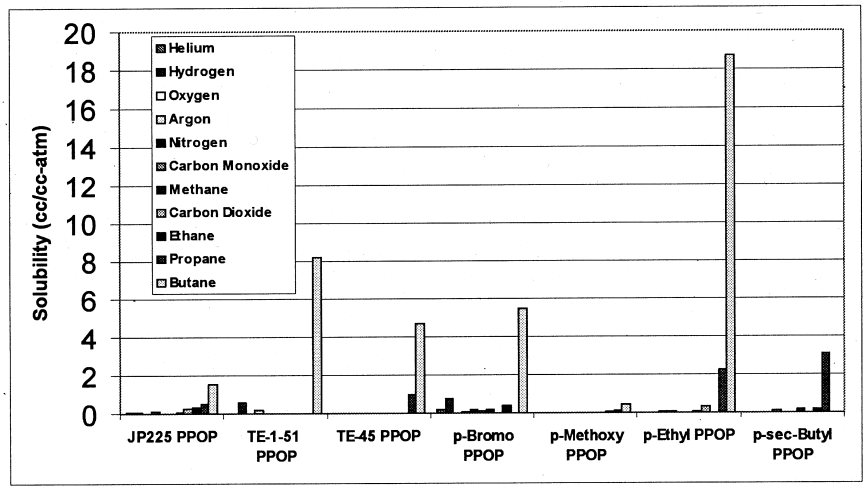

Figure 8. Solubilities of the test gases in the series of substituted phenoxy phosphazenes.

separations. The solubilities and diffusivities of the gases in the polymers series are shown in Figs. 8 and 9. The *p*-methoxy PPOP showed a selectivity in its permeation to helium, hydrogen, and carbon dioxide. Figs. 8 and 9 reveal that diffusion is mainly responsible for the helium and hydrogen permeabilities whereas the

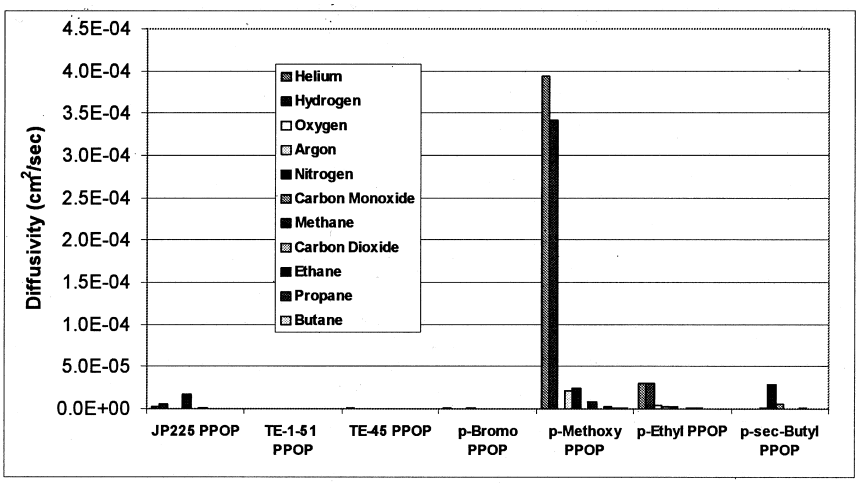

Figure 9. Diffusivities of the test gases in the series of substituted phenoxy phosphazenes.

MARCEL DEKKER, INC.
270 Madison Avenue, New York, New York 10016

higher carbon dioxide permeability is brought about by its increased solubility in the polymer. Also note the high solubility of the alkane gases in the polymers containing alkane moieties. The solubility of butane was very large for the *p*-ethyl PPOP and it actually dissolved the *p*-sec-butyl polymer. The polymer with the highest diffusivities of helium and hydrogen was the *p*-methoxy PPOP. This is the polymer which had the highest T_g.

The feed pressure dependence of the permeabilities for *p*-ethyl PPOP at 70°C are given in Fig. 10. It shows that there is no pressure dependence over the 20, 30, and 40 psia pressure range for this polymer for most of the gases. There does appear to be an increase in the permeability of butane as the feed pressure increases.

Recently a number of papers have been analyzing and developing a basis for the trade offs observed in small gas permeation properties (23-25). The majority of results show that in most cases as the permeability of a gas increases, the selectivity of that membrane to that gas decreases. Robeson (24) has collected the separation data for many gas pairs and plotted the observed selectivities verses permeabilities. The plot of the data suggested the well known upper bound for the data and finding a material that crossed over the line was unusual. A plot of the hydrogen permeabilty versus hydrogen/nitrogen selectivity for the series of polyphosphazenes studied in this work is shown in Fig. 11. The upper bound curve

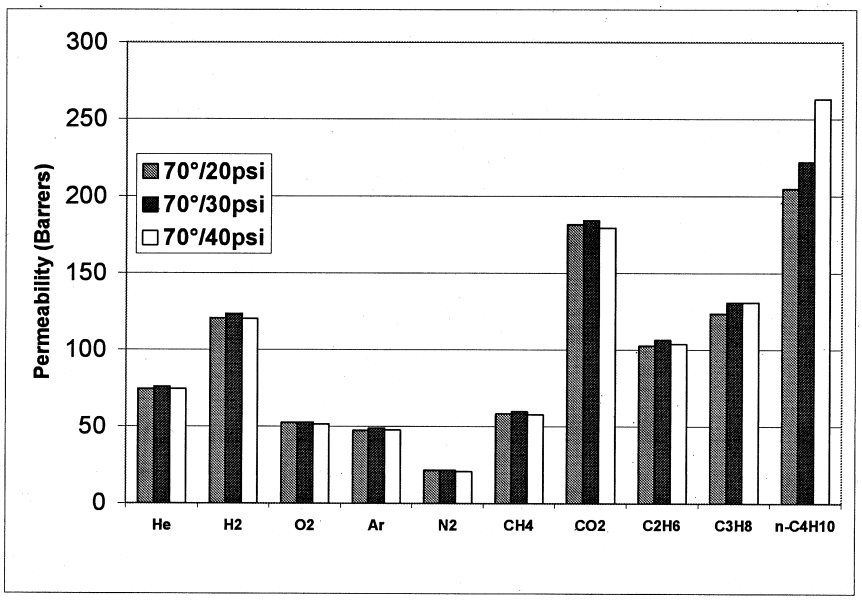

Figure 10. Pressure dependence of the permeability of *p*-ethyl PPOP.

MARCEL DEKKER, INC.
270 Madison Avenue, New York, New York 10016

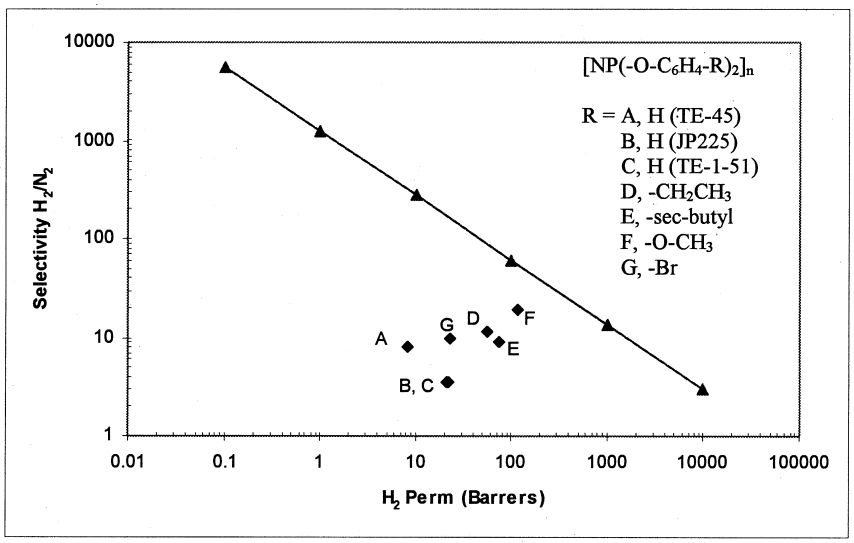

Figure 11. A log-log plot of H_2/N_2 selectivity versus H_2 permeabilities of the substituted bis phenoxyphosphazenes, showing the relation of these polymers to the Robeson upper limit curve (24).

was plotted using the Robeson values of k = 52918 and n = -1.5275 in the equation: line = $k^{-1/n}P^{1/n}$ given by Robeson. The plot shows that the polyphosphazenes follow the same pattern of behavior as do other polymers. However, one of the polymers (entry F), bis(*p*-methoxyphenoxy)phosphazene, is close to the line. When compared with the large number of polymers recorded by Robeson, the phosphazenes fall into the group of polymers having higher permeabilities and lower selectivities.

Freeman (25) provided an increased theoretical basis for the Robeson observations. Freeman concluded that the best pathway to improved performance is to both increase backbone stiffness and increase interchain separation. In the polymer series in this paper, the backbone remained constant and only the substituents were changed. Stern observed that the substitution of increasingly bulkier functional groups raises the glass-transition temperature, T_g, of polymers (23). The effects of such substitutions on the phosphazene polymers is illustrated in Fig. 12, which shows a plot of T_g versus the permeability to hydrogen for six of the polymers. A generic trend line shows that these polymers do not follow the pattern suggested by Stern. Polymers A (PPOP TE 1-45), B (PPOP JP225), and C (PPOP TE-1-51) in the figure are all bisphenoxy-substituted materials. The differences observed among these similar polymers may be due to the different amounts of

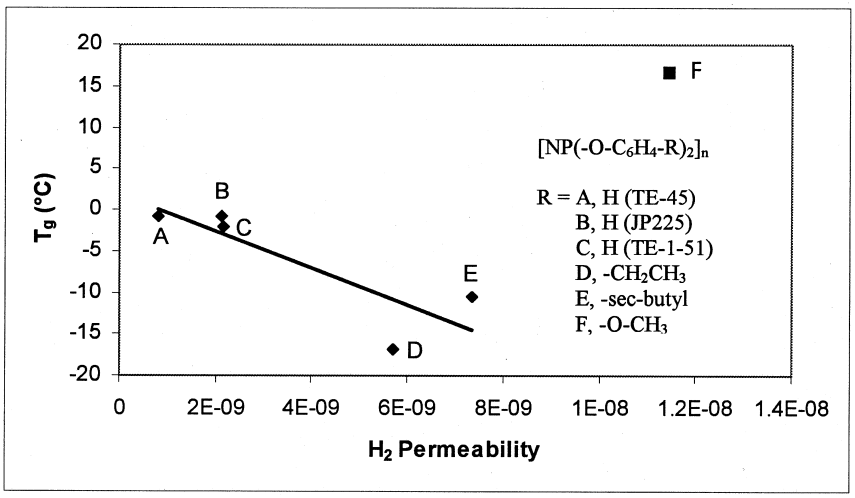

Figure 12. A plot of T_g versus hydrogen permeabilities for the substituted bisphenoxyphosphazenes. Due to ligand interactions, this series of polymers does not follow that seen in other materials.

crystallinity in the materials. D (*p*-ethylphenoxy) and E (*p-sec*-butylphenoxy) are substituted phenoxy materials that should be bulkier, but have T_gs lower than the parent compounds. The trend of increasing T_g with bulkier substituent holds on a very local level in that E is bulkier than D and does have a higher T_g. It is believed that the phenyl rings of the bisphenoxy materials tend to order through B-stacking. This would have the effect of decreasing the polymer mobility and give rise to the higher T_g. The subtituents on the phenoxy rings of samples D and E are apparently enough to prevent the phenyl rings from interacting. This would allow relatively more chain mobility and would thereby reduce the T_gs, as observed.

Even more anomalous is polymer F bis(*p*-methoxyphenoxy)phosphazene. It has a substantially higher T_g than the other polymers and also shows the highest permeability to hydrogen. This is the same polymer that was closest to the upper bound line in the H_2/N_2 Robeson plot. The polarity of the methoxy substituents must contribute to higher order by increased electrostatic interactions. These kind of interactions are not present in the alkane side groups that have lower T_gs.

CONCLUSIONS

A series of *p*-substituted bis phenoxy phosphazene polymers was synthesized. Membranes made from these materials were produced and tested in a single (pure) gas type of configuration. A wide variety of permeabilities were ob-

MARCEL DEKKER, INC.
270 Madison Avenue, New York, New York 10016

served and the solubility/diffusivity components reported. The unsubstituted phenoxy polymers were the least permeable to all of the gases. The substituted polymers showed different permeabilities relative to the individual gases tested. In some cases the pemeabilities were nearly all a diffusion controlled process, while for others, solubilities dominated. The permeabilities of some of the materials to CO_2 and the higher hydrocarbons was significant.

A Robeson type of plot of the selectivity versus permeability, shows that most of the phosphazenes fit into the more permeable group. It was observed that the T_gs of the whole series did not fit the usual pattern in that some of the materials with more bulky side groups actually had T_gs that were lower than the unsubstituted parent moieties. This result is proposed to be due to the ability of the phenyl rings of the phenoxy groups to stack and reduce chain mobility. The reason for the anomolously high T_g for the bis(*p*-methoxyphenoxy)phosphazene has not yet been fully resolved.

ACKNOWLEDGMENTS

This work was conducted at the Idaho National Engineering and Environmental Laboratory (INEEL) and it was supported by the U.S. Department of Energy, the Office of Industrial Technology, under Contract DE-AC07-99ID13727.

REFERENCES

1. R. W. Baker, E. L. Cussler, W. Eycamp, W. J. Koros, R. L. Riley, and H. Strathmann, *MEMBRANE SEPARATION SYSTEMS Recent Developments and Future Directions*, Noyes Data Corporation, Park Ridge, NJ, 1991.
2. Y. Sun, C. Lin, Y. Chen, and C. Wu, *J. of Membrane Science 134,* 117-126 (1997).
3. R. E. Singler, N. S. Schneider and G. L. Hagnauer, *Polym. Eng. Sci., 15*, 321-332 (1975).
4. P. Potin and R. De Jaeger, *Eur. Polym. J., 27*, 341-348 (1991).
5. F. F. Stewart, R. P. Lash, and R. E. Singler, *Macromolecules 30*, 3229-3233 (1997).
6. C. Rogers, J. A. Meyer, V. Stannett, and M. Szwarc, *TAPPI 39*, 737-747 (1956).
7. R. M. Barrer, Permeation, *Trans. Faraday Soc. 35,* 628-643 (1939).
8. G. J. van Amerongen, *J. of Applied Physics 17,* 972-985, (1946).
9. H. A. Daynes, *Proc. Roy. Soc. (London) A97,* 273 (1920).
10. G. Golemme and E. Drioli, *J. of Inorganic and Organometallic Polymers*, *6*, 341-365 (1996).
11. a) Ben-Amotz and Herschbach, *J. of Physical Chemistry 94*, 1044 (1990), b)

D. W. Van Drevelen, *Properties of Polymers*, Elsevier, 1990, c) A. S. Michaels and H. J. Bixler, *J. of Polymer Science L*, 413-439 (1961), d) Arthur M. Lesk, *Introduction to Physical Chemistry*, Prentice-Hall, Inc., Englewood Cliffs, N. J. 1982, e) J. O. Hirschfelder, C. F. Curtis, and R. B. Bird, *Molecular Theory of Gases and Liquids*, John Wiley & Sons, Inc., NY, 1954, and f) Donald W. Breck, *Zeolite Molecular Sieves*, Wiley-Interscience: NY, 1974.

12. E. Drioli, S.-M. Zhang, A. Basile, G. Golemme, S. N. Gaeta, and H.-C. Zhang, *Gas Separation and Purification 5*, 252-258 (1991).
13. R. R. McCaffrey, R. E. McAtee, D. G. Cummings, A. E. Grey, C. A. Allen, and A. D. Appelhans, *J. of Membrane Science 28*, 47-67 (1986).
14. R. R. McCaffrey and D. G. Cummings, *Separation Science and Technology 23*, 1627-1643 (1988).
15. E. S. Peterson, M. L. Stone, R. R. McCaffrey, and D. G. Cummings, *Separation Science and Technology 28*, 423-440 (1993).
16. E. S. Peterson, M. L. Stone, R. R. McCaffrey, and D. G. Cummings, *Separation Science and Technology 28*, 271-281 (1993).
17. E. S. Peterson, M. L. Stone, C. J. Orme, and D. A. Reavill III, *Separation Science and Technology 30*, 1573-1587 (1995).
18. M. Kajiwara, *J. of Materials Science 29,* 6268-6272 (1994).
19. M. Kajiwara, *Separation Science and Tehcnolog 26*, 841-852 (1991).
20. M. Kajiwara, *J. of Materials Science 23,* 1360-1362 (1988).
21. G. Golemme, E. Drioli and F. Lufrano, *Polymer Science 36*, 1647-1652 (1994).
22. H. R. Allcock, C. J. Nelson, W. D. Coggio, I. Manners, W. J. Koros, D. R. B. Walker and L. A. Pessan, *Macromolecules 26*, 1493-1502 (1993).
23. S. Alexander Stern, *J. of Membrane Science 94,* 1-65 (1994).
24. Lloyd M. Robeson, *J. of Membrane Science 62,* 165-185 (1991).
25. Benny D. Freeman, *Macromolecules 32,* 375-380 (1999).

MARCEL DEKKER, INC.
270 Madison Avenue, New York, New York 10016

Request Permission or Order Reprints Instantly!